

hemisphere. Since this change occurs in the energy region of the second nucleon isobar, $N^*(1512)$, it may perhaps be due to an interference between the rapidly varying resonant amplitude and nonresonant states of opposite parity.

We wish to thank Professor Luis W. Alvarez for his

encouragement and advice. Theoretical consultations with Professor Gyo Takeda and Professor A. Charles Zemach have been most useful. The enthusiastic help of our data analysts, especially Jerry H. Friedman, Joe F. Hanna, C. Tom Owens, and Jack Weinberg, is gratefully acknowledged.

Extrapolation Methods and the Nucleon-Deuteron Breakup Reaction*

I. J. R. ATCHISON

Brookhaven National Laboratory, Upton, New York

(Received 15 February 1963)

The Chew-Low extrapolation as applied to the nucleon-deuteron breakup reaction is studied. Singularities of the amplitude and cross sections are located using perturbation theory and simple final-state interaction theory. The measured cross sections, whose kinematic singularities are exhibited, are expressed in terms of the invariant Chew-Low cross sections. The experimental procedure is outlined, and forms are suggested for the fitting curves.

1. INTRODUCTION

SINCE the paper of Chew and Low,¹ single-particle exchange models have been much exploited. One of the applications they suggested was to the determination of n - n scattering observables from n - d scattering: The differential or total n - n cross section could be found from the residue of a pole in the corresponding cross sections for the process $n+d \rightarrow n+p+n$. Some indication as to the practicality of this idea can be found by looking at the analogous reaction $p+d \rightarrow n+p+p$, using it to determine, in this way, the (known) p - p cross sections. This experiment is being done by Griffiths and Batty,² using the 30–50 MeV LINAC at the Rutherford Laboratory, Harwell. A modified Chew-Low procedure has already been used by Kuckes *et al.*,³ and agrees qualitatively with the data.

The pole, which is of second order, occurs in a momentum transfer variable Δ^2 ; there is also a first-order pole at the same point. Apart from these, the cross section is, for purposes of extrapolation, usually expressed as a polynomial in Δ^2 . But this is only justified if there are no other singularities in Δ^2 inside a circle, whose center is the Chew-Low pole, including a substantial part of the physical region. In other words, it will be difficult to separate out the effect of the single-particle exchange term if other processes are equally important in the same region of phase space: Rather, one ought to include terms in the extrapolation, or fitting, curve—for

instance, additional poles—to take account of these processes.

The possibility of such singularities is something that can be examined, to some extent, theoretically. For example, Landshoff and Treiman⁴ have pointed out that a three-point graph (see Sec. 3) could prejudice the determination of the $\pi\pi$ cross section from the $\pi p \rightarrow \pi\pi p$ data. The first step is to locate the singularities of the amplitude T ; this is done in Sec. 3, in which poles, 2- and 3-point graphs are analyzed, and contributions from final-state interactions considered. In Sec. 4 the cross sections are defined in terms of T , and some of their singularities found.⁵ Sections 3 and 4 use the kinematical results of Appendix A, which are dealt with descriptively in Sec. 2.

The conclusion of this analysis, so far as it goes, is that certain regions of phase space are likely to be “dangerous,” being strongly influenced by final-state interactions. In Sec. 5 we show how to avoid these regions, treating in particular Griffith’s experiment. Kinematical singularities are eliminated, and suggestions offered on the form of extrapolation curve to be used near the dangerous regions. No account of polarization effects is given.

2. NOTATION AND KINEMATICS

A.

For the five-particle process [Fig. 1(a)]

$$1+6 \rightarrow 3+4+5$$

there are ten possible scalar products $p_i p_j$ ($i \neq j$) which

⁴ P. V. Landshoff and S. B. Treiman, *Nuovo Cimento* **19**, 1249 (1961).

⁵ I. T. Drummond, in a preprint received after this work was done, has also considered this problem.

* Based, in part, on a thesis submitted to Cambridge University for the degree of Ph.D. Work performed partially under the auspices of the U. S. Atomic Energy Commission.

¹ G. F. Chew and F. E. Low, *Phys. Rev.* **113**, 1640 (1959), referred to as C-L.

² R. J. Griffiths and C. J. Batty (private communication).

³ A. F. Kuckes, R. Wilson, and P. F. Cooper, Jr., *Ann. Phys.* (N. Y.) **15**, 193 (1961).

we may choose as variables. Only five are linearly independent though, the remainder being redundant, corresponding to there being five degrees of freedom in the final state after conservation of over-all four-momentum is satisfied. We choose the independent variables to be [the metric is (1-1-1-1)]

$$W^2 = (p_1 + p_6)^2, \quad \Delta^2 = (p_5 - p_6)^2, \quad Q^2 = (p_3 + p_5)^2, \\ s = (p_3 + p_4)^2, \quad t = (p_4 - p_1)^2$$

which will be called collectively (\mathcal{G}). The C-L pole is at $\Delta^2 = m^2$, where m is the nucleon mass; it is illustrated in Fig. 1(b).

In Griffith's experiment, the incoming nucleon has a laboratory energy of 30 MeV, so nonrelativistic variables are adequate, once the analysis of singularities has been done in terms of the (\mathcal{G}). The set of five nonrelativistic variables will be called (\mathcal{X}). Denote by q_1 the magnitude of the momentum of 1, by p that of the recoil particle 5 (both in the lab system in which the deuteron, particle 6, is at rest), and by \mathbf{Q} the relative momentum of 3 and 5 in their c.m. system. If z and \mathbf{q} are the cosine of the scattering angle and relative momentum of particles 3 and 4 in their c.m. system, (\mathcal{X}) is the set $(q_1^2, p_1^2, \mathbf{Q}^2, |\mathbf{q}^2|, z)$. (\mathcal{X}) and (\mathcal{G}) are related by

$$Q^2 = 4m^2 + 4\mathbf{Q}^2, \quad \Delta^2 = m^2 - 2(p^2 + \alpha^2), \quad s = 4m^2 + 4q^2, \\ W^2 = 9m^2 - 6\alpha^2 + 2q_1^2, \quad (1) \\ t = -2q^2 - p^2 - \alpha^2 + 2qz(p^2 + q^2 + \alpha^2)^{1/2}.$$

Here $q^2 = |\mathbf{q}^2|$, and the deuteron mass is $2m - \alpha^2/m$; α^2/m is the deuteron binding energy.

Since the C-L pole is at $p^2 = -\alpha^2$, it is useful to define the dimensionless variable $x = (p^2 + \alpha^2)/q_1^2$. The x plane is a more convenient scale than the Δ^2 plane for discussing the positions of singularities in relation to the physical region, which we now describe.

B.

Although the variables (\mathcal{G}) or (\mathcal{X}) are independent, physical restrictions on energies and angles place limits on their values. We mention two reasons why we must learn something about the allowed physical regions. First, the limits on p^2 are especially important. The maximum range of p^2 is $0 \leq p^2 \leq q_1^2$, while the C-L pole is at $p^2 = -\alpha^2 \approx q_1^2/30$. Hence, for the extrapolation, we

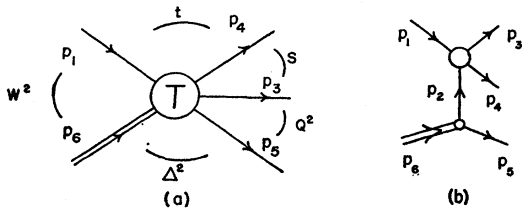


FIG. 1. (a) T is the amplitude. p_1 and p_6 are the four-momenta of the incoming nucleon and deuteron, respectively; p_3 , p_4 , and p_5 are those of the outgoing nucleons. (b) The C-L pole at $(p_5 - p_6)^2 = p^2 = m^2$. Particle 5 is the "recoil" particle having momentum \mathbf{p} in the laboratory system.

want experimental points particularly in the region of low p^2 . It follows that we must know how to ensure that this region is accessible for a particular experiment. For instance, C-L already pointed out that, for a given q^2 , only part of the full p^2 range is attainable. We shall recall this point below, and also further delimit the range of p^2 .

Second, in Secs. 3 and 4 some singularities are analyzed. We are interested in their positions in the Δ^2 or x planes, but they will, in general, depend on some or all the other four of the (\mathcal{G}). So we must know what are the ranges of all the variables for a physical process, so that the nearest and furthest distances of approach of the singularities to the C-L pole may be found. The idea is then to choose experimentally a region of phase space such that what seem to be the worst singularities are not too close to the C-L pole. To do this, the preferred region of (\mathcal{G}) or (\mathcal{X}) space must be translated into a region of laboratory phase space, since none of Q^2 , t , or q^2 , for example, are measured directly; this is done in Sec. 5.

Let E_i be the lab energy of particle i , and z_{ij} the cosine of the lab angle between i and j , the polar axis being taken along the direction of q_1 . Equation (A1) and the requirement $|z_{i6}| \leq 1$ give the C-L phase diagrams (Figs. 1 and 2 of reference 1) for p^2 and q^2 . For $q^2 = q_0^2 = \frac{1}{4}q_1^2 - \alpha^2$, the allowed p^2 region is $0 \leq p^2 \leq (4/9)q_1^2$; this is the only value of q^2 for which $p^2 = 0$ is attainable, and so is the "best" q^2 to choose experimentally, since the region $p^2 \approx 0$ is of especial interest.

We consider now other limitations on the values of p^2 . Since \mathbf{p}_3^2 must be non-negative, from (A5) it follows that

$$p^2 \leq 2Q^2 - t/2, \quad (2)$$

and since the momentum transfer $(p_1 - p_5)^2$ is non-positive

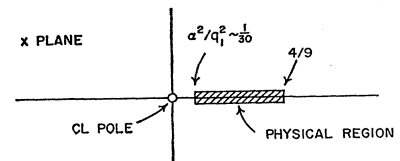
$$p^2 \geq -2q^2 - t/2 - \alpha^2. \quad (3)$$

The condition $|z_{13}| \leq 1$ is expressed in (A7), where we have taken $q^2 = q_0^2$. Neglecting α^2 , putting $u = 2\mathbf{Q}^2$, $v = 3p^2$, $w = 3t/2$, and scaling by q_1^2 , (A7) may be written as

$$-\frac{2}{3}[6u+1]^{1/2} \leq (v-u+w+\frac{2}{3}) \leq \frac{2}{3}[6u+1]^{1/2}. \quad (4)$$

The planes $v, w = \text{constant}$ cut the region (4) in parabolas. Combining these results, the maximum extent of the physical region of p^2 is given by the C-L diagram; the actual upper limit on p^2 is the value from Fig. 1, Eq. (2) or (4) whichever is the least [the limit (4) is weaker than (2) provided $\mathbf{Q}^2 \leq \frac{1}{4}q_1^2$], while the lower limit is the largest of (3), (4), and Fig. 1. Figure 2 shows,

FIG. 2. The C-L pole is at $x=0$; the maximum extent of the physical region if $\alpha^2/q_1^2 \leq x \leq (4/9) + (\alpha^2/q_1^2)$.



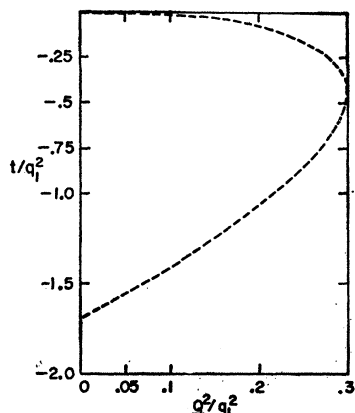


FIG. 3. The area enclosed by the dashed line and the t/q_1^2 axis is the physical region.

in the x plane, the C-L pole and the maximum extent of the physical region for $q^2 = q_0^2$.

We can also obtain phase diagrams linking other variables. The restriction $|z_{14}| \leq 1$ is expressed by (A8), and solving for t gives the $t-Q^2$ diagram of Fig. 3. Finally, since $\mathbf{q}_1 - 3\mathbf{p} = 4\mathbf{Q} - 2\mathbf{q}$, using (A1) and the condition $|\cos(\mathbf{Q}, \mathbf{q})| \leq 1$, we get the Q^2-q^2 diagram of Fig. 4. In particular, at $q^2 = q_1^2$, $0 \leq Q^2 \leq \frac{1}{4}q_1^2 - \frac{1}{2}\alpha^2$. These diagrams show the interconnection between allowed values of p^2 , Q^2 , q^2 , and t .

C.

As we mentioned in Sec. 2A, of the ten possible scalar invariants only five are linearly independent; we chose five of the form $(p_i \pm p_j)^2$, the set (g) . We call the remaining five such products S_{ij} [the relations between them and the (g) are given in (A9)–(A13)]. Three of the S_{ij} involve Δ^2 directly: This means that singularities in one of these are effectively singularities in Δ^2 , as Landshoff and Treiman have pointed out.⁴

A dependence more complicated than linear is found if we choose a nonvariant variable as one of the independent five. Two examples arise. First, suppose we want to know the singularities of the partial cross section $\partial\sigma/\partial s \partial t \partial \Delta^2 = \sigma_3$. σ_3 is obtained from $\sigma_4 = \partial\sigma/\partial s \partial t \partial \Delta^2 \partial Q^2$ by a single integration, and the singularities of σ_4 are just those of $|T|^2$, apart from kinematical factors. For σ_3 there is one less degree of freedom, so

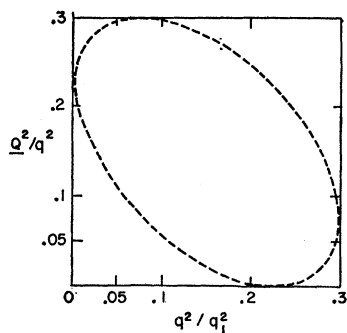


FIG. 4. The area inside the ellipse is the physical region.

that one of the (g) —namely, Q^2 —is redundant. The integration involved can be written as one over either Q^2 or an angle variable, such as the relative azimuthal angle φ of particles 3 and 5 in the c.m. system of 3 and 4. In the first case the range of integration—the physical region of Q^2 when s , t , and Δ^2 are given—has to be found. This is most conveniently done by expressing Q^2 in terms of s , t , Δ^2 , and $\cos\varphi$, for then the condition $|\cos\varphi| \leq 1$ gives the Q^2 range. [See (A15').] But it is awkward to have Δ^2 appearing in the limits, since it is in that variable that we are interested in the properties of σ_3 . Instead, we may integrate over φ rather than Q^2 , in which case the limits are simple, but Q^2 has to be replaced by (A15'). One can then find the singularities of σ_3 by considering how those of the integrand move in the φ plane as Δ^2 is varied. Similarly, for $\sigma_2 = \partial\sigma/\partial s \partial \Delta^2$, t as well as Q^2 has to be integrated over. By expressing t in terms of s , Δ^2 , and $\cos\theta$, the cosine of the scattering angle of 3 and 4 in their c.m. system, by (A14), σ_2 is written as a double integral over θ and φ .

Second, the experimental arrangement may limit the number of degrees of freedom. For Griffith's experiment, all particles are coplanar, so that the restriction $\varphi_{34} = \pi$ is imposed, where φ_{34} is the relative azimuthal angle of 3 and 4 in the lab system. Now only four variables are independent. The cross section of interest is related to $\partial\sigma_3/\partial\varphi_{34}$ with $\varphi_{34} = \pi$. Hence, Q^2 is no longer a free variable and has to be expressed as a function of s , t , Δ^2 , and φ_{34} . [See (A19).] We shall see in Sec. 3 that singularities in Q^2 and the related variables S_{45} are just the important ones; in Q^2 they occur at $Q^2 \approx 0$, so that in (A20) and (A21) we have taken $Q^2 = 0$ to simplify the equations.

The main purposes of these considerations is to stress that in the analysis of Sec. 3 we have to be careful to include all singularities in variables that are not independent of Δ^2 .

3. SINGULARITIES OF THE BREAK-UP AMPLITUDE

A.

For definiteness we shall consider the process $p+d \rightarrow p+n+p$. There are nine single-particle exchange poles occurring when the initial and final particles can be formed into two groups, each with the quantum numbers of a single particle.¹ One is the C-L pole at $\Delta^2 = m^2$ (or $x=0$); another is the pole in W^2 at the helium mass, which is independent of Δ^2 . We list the other seven, the positions being evaluated for $q^2 = q_0^2$.

The only poles involving Δ^2 directly [cf., (A9)–(A13)] are those at $S_{15} = \mu^2$, $\bar{t} = \mu^2$, and $S_{36} = m^2$, where μ is the pion mass. The first is at $x \sim 0.7$, and the second is at $x = -\frac{1}{2}\mu^2 = 2q^2 - t/2$. The nearest approach to $x=0$ is found by choosing $t = -4q^2$ (the least value of t allowing an extrapolation to real z at $x=0$), in which case its position is $x \sim \frac{1}{6}$. For $t=0$ it is at $x \sim 0.8$. The pole $S_{36} = m^2$ is at $p^2 = 2Q^2 - t/2 + \alpha^2$. From Eq. (2) this is

just α^2 from the upper limit of the physical p^2 range. It is of the same type as the C-L pole, α^2 below the physical region.

The remaining poles involve Δ^2 only when one or both of t and Q^2 is not a free variable. σ_2 and σ_3 are considered in more detail in Sec. 4; for the moment we note the singularities for the cases $z=0, \pm 1, \cos\varphi = \pm 1$. Neglecting α^2 , the pole $Q^2 = m_a^2$ is [A(15)] at $x = \frac{1}{6}$ for $\cos\varphi = 1, z=0$, while for $z=1, -1$ it is at $x=0$ and $4/9$, respectively. The position of the $S_{45} = m_a^2$ pole is found by interchanging the sign of z and $\cos\varphi$. As z varies, the $t = \mu^2$ pole describes an arc of a circle in the x plane; its nearest distance from $x=0$ is at $x = \pm 1$, for which it is at $x = -\mu^2 \pm 2\mu q_1$, $|x| \sim 0.7$. The pole $\bar{t} = \mu^2$ is found by changing the sign of z . For $z = \pm 1$ and $Q^2 = 0$ the pole $S_{36} = m^2$ is at $x = 2\alpha^2/q_1^2$ [Eq. (A15')] and for $z = \pm 1$ it is the pole $S_{46} = m^2$ which is at $x = 2\alpha^2/q_1^2$ when Q^2 has its maximum value ($\frac{1}{4}q_1^2 - \alpha^2/2$ when $q^2 = q_0^2$, according to Fig. 4).

For the case in which 3 and 4 are coplanar, similar results hold. Using (A22) and (A23) to express Q^2 in terms of p^2, q^2 , and z one finds that the S_{36} and Q^2 poles are at $x=0$ for $z=-1$, and the S_{46} and S_{45} ones are at $x=0$ for $z=1$. For $z=0$, the Q^2 and S_{45} poles are at $x \sim \frac{1}{6}$ (A20) while those in S_{36} and S_{46} appear at the roots of the cubic $4x^3 + 0.92x^2 - 1.52x + 1 = 0$. The cubic has one real root $x \sim 0.9$, and two complex roots, $|x| \sim 0.5$.

We see that some single particle poles may be close to, or on top of, the C-L pole when the variables involved are at the limits of their ranges. However, neither the S_{36} nor the S_{46} pole should be important in an experiment which selects events in which 5, rather than 3 or 4, is a spectator; and we shall see below (Sec. 3C) that the Q^2 and S_{45} poles, corresponding to triplet-state interactions, are much less important than terms accounting for singlet-state interactions. In any case, all these singularities could be included explicitly in the fitting curve.

B.

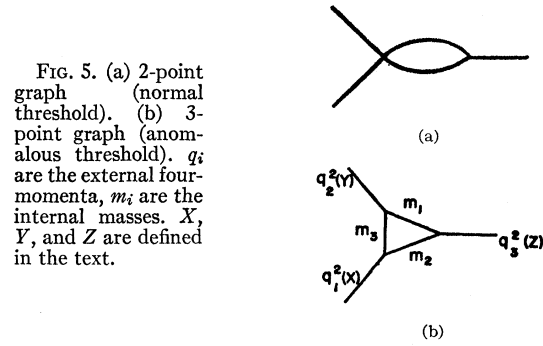
The next lowest order perturbation theory graphs are the 2- and 3-point graphs of Figs. 5(a) and (b); the singularities of the latter include those of the former. Both graphs lead to branch points rather than poles; Fig. 5(a) of the square root, Fig. 5(b) of the logarithmic type.

A full description of the relevant properties of 3-point graphs has been given by Bonnevey *et al.*⁶ which contains appropriate references. Application to the present problem is discussed, and only the results are given here. Defining

$$q_1^2 = m_2^2 + m_3^2 - 2m_2m_3X,$$

and cyclically for Y and Z in terms of q_2^2 and q_3^2 , the branch points from Fig. 5 are at $X, Y, Z = -1$. As well

⁶ G. Bonnevey, I. J. R. Aitchison, and J. S. Dowker, *Nuovo Cimento* 21, 1001 (1961).



as these normal thresholds, the amplitude T represented by Fig. 1 may also have branch points—*anomalous thresholds*—at points on the surface Σ given by

$$X^2 + Y^2 + Z^2 - 2XYZ - 1 = 0.$$

Reference 5 established which of these points are singular on the physical sheet: As a first orientation, it is these ones that are expected to be important physically.

In our case, at least one of the q_i , say q_3 , in Fig. 5(b) must represent a stable particle: This means that Z is real, say $Z = a, -1 \leq a \leq 1$. In the subsequent analysis, we examine only graphs in which one or both of Y and Z represent either Δ^2 itself or an S_{ij} related to Δ^2 ; the case in which t or Q^2 is not a free variable is not discussed. Hence, this section applies directly only to the singularities of σ_4 . Also, all positions will be evaluated at $q^2 = q_0^2$.

To apply the rules of Bonnevey *et al.*⁶ systematically we must enumerate the 3-point graphs occurring in the process of Fig. 1. Of the cases in which two external lines represent real particles, variables Y and Z , only those four need be considered in which the invariant belonging to the third line is one of $(1\bar{1}), (6\bar{6}), i=3,5$, since the others do not involve Δ^2 ; the shorthand (ij) stands for the invariant associated with particles i and j , a bar denoting a negative four-momentum. Typical graphs are shown in Figs. 6(a)–(c). The first two have only normal thresholds. For Fig. 6(a), the branch point is at $x = 2\mu^2 + 2q^2 + t/2$ for $i=3, x = 2\mu^2 - \alpha^2 + 1 - 2q^2$ for $i=5$. The second is fixed, at $x \sim \frac{5}{6}$, while the first is at $x > \frac{2}{3}$ for $t \geq -4q^2$. For Fig. 6(b) the branch points are at $x \sim \pm 2m^2 = 30$, very far from $x=0$, illustrating the general point that the normal thresholds nearest to the physical region are those associated with the lowest

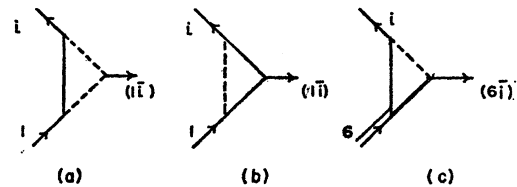


FIG. 6. In this and subsequent graphs, the dashed lines represent pions, the solid ones nucleons, and the double line is the deuteron.

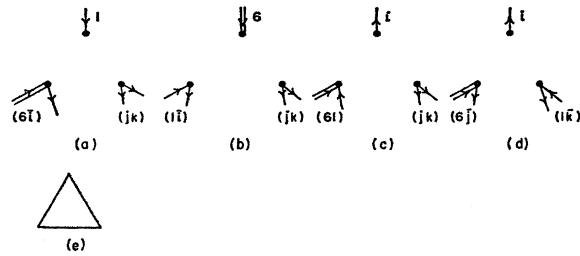


FIG. 7. (a)-(d) Possible configurations of the five external lines at the vertices of a 3-point graph. (e) Structure of intermediate states in a 3-point graph.

mass intermediate states. Figure 6(c), on the other hand, has the usual anomalous threshold associated with the deuteron vertex.⁷ For $i=3$, the branch point is at $x = \frac{1}{2}(\mu^2 + 0.35m\mu + 4\alpha^2 + 4Q^2 - t)$, which reaches $x=0.6$ for $t=Q^2=0$. For $i=5$ it is at $x=-0.6$. The normal thresholds are both far away, $|x| \sim 2.5$.

The remaining graphs are those in which only one external line represents a real particle. The possible configurations of the external lines are shown in Figs. 7(a)-(d). Figure 7(c) does not have to be considered as it does not involve Δ^2 , and the same is true for (a) and (b) for $i=4$. We then have to insert the lowest mass intermediate states with the structure of Fig. 7(e), consistent with the conservation laws. The nearest normal thresholds have already been discussed: It remains to analyze the anomalous thresholds.

It turns out that only two three-point graphs can cause trouble. For the others, the kinematics of the physical regions imply that Σ is either not singular on the physical sheet, or else the singular points are far from $p^2 \approx 0$. One comes from contracting the line l in Fig. 8. For the maximum allowed Q^2 , the singularity is at $x = -0.5 - t/2$. From (A8) we see that t has the range $-\frac{1}{4}q_1^2 - \frac{2}{3}\alpha^2 \geq t \geq -q_1^2 + 2\alpha^2$ for this Q^2 , so that it approaches very close to $x=0$. The maximum Q^2 corresponds to the production threshold for 4 and 5 in the final state. The other graph is the same with 3 and 5 exchanged, for which $x \approx 0$ is reached at $Q^2=0$, the threshold for producing 3 and 5 in the final state.

These graphs may be interpreted as final-state interactions,⁸ and could well be important. However, they represent the effect of a point interaction at the (45) or (34) vertex. The singularity we have found is most important in the phase-space region in which 4 and 5

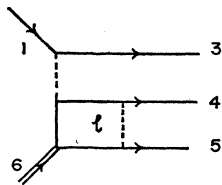


FIG. 8. "Final-state interaction" graph.

⁷ R. Karplus, C. M. Sommerfeld, and E. H. Wichmann, Phys. Rev. **111**, 1187 (1958).

⁸ R. F. Sawyer, Phys. Rev. Letters **7**, 213 (1961).

(or 3 and 4) have nearly zero relative momentum, which is just the region in which the nucleon-nucleon cross section rises very sharply. It is more likely that the main final-state effect is this low-energy "resonance," which we now consider.

C.

We recall that we are trying to separate out the effects of the C-L pole which, in the reaction $p+d \rightarrow p+n+p$, is important when the energy of the n is low. Now, there are also processes leading to a slow proton in the final state: The incoming proton may collide with either target particle and only just dissociate the d , or it may exchange with the target proton having transferred most of its energy to it. In these cases, since the low-energy $n-p$ cross section rises sharply, the effect of the C-L pole may be masked.

There is evidence that this is so. For an incident proton energy of 9 MeV, Nakada *et al.*⁹ have measured the cross section $\bar{\sigma}_2 = \partial\sigma/\partial E'\partial\Omega'$ where Ω' is the solid angle around \mathbf{p}' , the momentum of the recoil n in the over-all c.m. system, and $E' = p'^2/2m$. $\bar{\sigma}_2$ is related to σ_2 , using (A13). At 0° , the spectrum $\partial\sigma/\partial E'$ shows two pronounced peaks, at low and high neutron energies. A simple calculation shows that the position of the low-energy peak is not correctly given by the C-L term which peaks too near $E'=0$, although one can perhaps distinguish a small shoulder corresponding to it. A detailed calculation by Komarov and Popova¹⁰ including both $p-p$ and $n-p$ final-state interactions gives good agreement, the high-energy peak being ascribed to the $p-p$ interaction. So, at least for σ_2 , singularities from processes other than the C-L pole are of greater weight than it.

It is desirable to have a simply analytic expression to represent these effects. Such a form was proposed by Watson,¹¹ and has been re-examined by McVoy.¹² These authors suggest that the final-state interaction of 3 and 5 can be represented by a term in the amplitude

$$f = [e^{i\delta} \sin\delta / |Q|] \times (\text{factors varying slowly with } |Q|),$$

where δ is the 3-5 phase shift. If we assume that only the scattering length a enters, f can be written as $F/(i|Q| + a^{-1})$, where F varies slowly with $|Q|$. The main singularity is then a pole in the Q^2 plane at $-a^{-2}$. Notice that f satisfies unitarity, and has the right threshold behavior at $Q^2=0$.

For a detailed critique of this assumption for f we refer to references 11 and 12, remarking only that the essential criterion for its validity—that the scattering cross section be large compared with the cross section of the region of interaction—is well satisfied in this case,

⁹ M. P. Nakada, Phys. Rev. **110**, 595 (1958).

¹⁰ V. V. Komarov and A. M. Popova, Zh. Eksperim. i Teor. Fiz. **38**, 1559 (1960) [translation: Soviet Phys.—JETP **11**, 1123 (1960)].

¹¹ K. M. Watson, Phys. Rev. **88**, 1163 (1952).

¹² K. W. McVoy, Phys. Rev. **121**, 1401 (1961).

especially for singlet scattering. There are other indications that it is reasonable. The n - p singlet scattering length a_s is much larger than the triplet one, a_t : $a_s \sim -20$ F, $a_t \sim 5$ F.¹³ It follows that the pole $\mathbf{Q}^2 = -a_s^{-2}$ is closer to the physical region than that at $-a_t^{-2}$, corresponding to the results of reference 10. If we neglect a_s^{-2} , the point $\mathbf{Q}^2 = 0$ is at $E' \sim 0.65$ MeV for forward scattering, just the position of the low-neutron energy peak in Nakada's data.⁹ Also, the position and width of the high-energy peak are very well given by taking this form for f , with a singlet p - p scattering length of -5.5 F.¹⁴ Indeed, Ilakovac *et al.*¹⁵ have used this approximation to determine the n - n scattering length from the reaction $nd \rightarrow nnp$, as Singh had proposed earlier.¹⁶

Singh has shown¹⁶ that the contribution of the plane wave part of the final-state wave function is only about one seventh of that including interactions. Some idea of the relative magnitudes can be got by considering a point-interaction model. A calculation similar to that of Karplus and Rodberg,¹⁷ for example, implies that the amplitude for the process in which the incoming proton hits the target proton, which then interacts with the neutron, is proportional to

$$A = f_{pp} \frac{\alpha^{1/2}}{\pi} \left\{ \frac{1}{p^2 + \alpha^2} + \frac{if_{np}(|\mathbf{Q}|)}{|\mathbf{q}_3 + \mathbf{p}|} \right. \\ \left. \times \ln \left[\frac{(|\mathbf{q}_3 + \mathbf{p}|/2) + |\mathbf{Q}| + i\alpha}{(|\mathbf{q}_3 + \mathbf{p}|/2) + |\mathbf{Q}| - i\alpha} \right] \right\}, \quad (5)$$

where f_{pp} , f_{np} are the p - p and n - p amplitudes, respectively, $f_{np} = -(i|\mathbf{Q}| + \alpha^{-1})^{-1}$ and the deuteron wave function is $(\alpha^{1/2}/\pi)e^{-\alpha r}$. The first term of A (the plane wave part) is just the C-L pole; the second is the final state interaction. The singularities of the logarithm are exactly those of the corresponding 3-point graph discussed earlier, but the main $|\mathbf{Q}|$ dependence certainly comes from f_{np} . At $|\mathbf{Q}| = 0$, $f_{np} = -a_s$ (taking only the singlet interaction) so the second term in A is $-(ia_s/2p) \ln[(p+i\alpha)/(p-i\alpha)]$, so the logarithm is pure imaginary. At $E' \sim 0.65$ MeV, taking \mathbf{p}' along \mathbf{q} , the second term is roughly nine times the first, and of the same sign (for the triplet interaction, the opposite sign if a_t would lead to destructive interference). Of course the over-all effect is not so pronounced, since for $\bar{\sigma}_2$ we integrate over the angles between \mathbf{q} and \mathbf{p}' : For example, at $\mathbf{p} = 0$, corresponding to $\cos(\mathbf{q}, \mathbf{p}') \sim 90^\circ$ and $E' = 1$ MeV, the two terms are roughly equal. Nevertheless, it is clear that the pole is masked.

¹³ J. M. Blatt and V. Weisskopf, *Theoretical Nuclear Physics* (John Wiley & Sons, Inc., New York, 1952), p. 71.

¹⁴ H. P. Noyes and D. Wong, *Phys. Rev. Letters* **3**, 191 (1959).

¹⁵ K. Ilakovac (unpublished).

¹⁶ L. S. Singh, thesis, University College, London University, 1959.

¹⁷ R. Karplus and L. S. Rodberg, *Phys. Rev.* **115**, 1058 (1959).

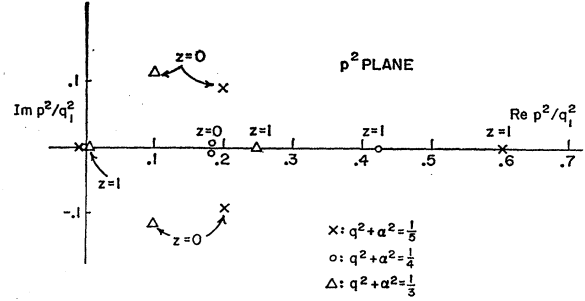


FIG. 9. The positions of the final-state interaction pole for various q^2 and z .

This also emerges from considering how the pole in f_{np} moves in the x plane, which it is necessary to do for σ_3 and σ_2 , and if 3 and 4 are coplanar. We treat the coplanar case as an example, taking $a_s^{-2} \approx 0$. Using (A24) with $q^2 = q_0^2$, neglecting α^2 , we find that it is at

$$x = (3 + z^2)/18 \pm (15 + z^2)^{1/2}/18,$$

so that it goes from 0 to 4/9 as z goes from -1 to 1 (the points move off the physical region if α^2 is included). Equation (A24) can also be solved for different q^2 ; the results for $q^2 = \frac{1}{3}, \frac{1}{4}, \frac{1}{5}$ are shown roughly in Fig. 9. It is clear that this singularity is near the physical region, and can be dangerously close to the C-L pole. The value $q^2 = \frac{1}{5}$ is slightly more favorable than q_0^2 , since it allows larger z 's to be used. As q^2 decreases the lowest allowed p^2 increases, but it is still low enough at $q^2 = \frac{1}{5}$ to make it worth considering doing the experiment at this value.

It is suggested then that the 3-point singularity—that of the logarithm in (5)—is less important than the pole of f_{np} . The total amplitude T is antisymmetric in 3 and 4, so that the final-state interaction part has the form

$$\left(\frac{1}{i|\mathbf{Q}| + a_s^{-1}} - \frac{1}{\frac{1}{2}i|\mathbf{p}_4 - \mathbf{p}| + a_s^{-1}} \right) \\ \times \text{factors slowly varying.} \quad (6)$$

The positions of the pole in the second term of (6) may be found from those of the first by interchanging the sign of z .

4. SINGULARITIES IN THE CROSS SECTIONS

A collection of singularities of the amplitude has been discussed; to justify an extrapolation of observed data, we have to show that the corresponding cross section has a large enough radius of convergence about the C-L pole. This has first to be defined so that it is an analytic function. In the physical region, where all variables are real, the total cross section is essentially

$$\sigma = \int |T|^2 d\tau, \quad (7)$$

where $d\tau$ is the phase-space element and T is the total amplitude. But we must not use (7) to define σ everywhere, since T^* , the complex conjugate of T , is not an analytic function; rather, the definition must coincide with (7) in the physical region while allowing continuation away from it.

We illustrate the definition to be adopted by considering the examples of the singularities treated in Sec. 3. For poles, σ is easily defined. Consider the term $(t^2 - \mu^2 + i\epsilon)^{-1}$, in which ϵ is a small positive number tending to zero (the Feynman prescription for satisfying causality). In the physical region, the denominator never vanishes, so ϵ can be put equal to zero, and the contribution to σ is

$$\sigma^{14} = \int [1/(t - \mu^2)^2] d\tau$$

which also defines σ^{14} off the real axis. For the triangle graphs ϵ is important, though. Suppose for some such amplitude F , Z is associated with a stable particle vertex, Y with an energy variable and X with a momentum transfer variable. In the physical region, $-1 < Z < 1$, $Y \leq -1$, $X \geq 0$. Since Y is on the cut which starts from the normal threshold $Y = -1$, we have to consider $F_{ppp}(X, Y - i\epsilon, a)$ as $\epsilon \rightarrow 0$; the suffixes $p(u)$ on F mean that the variables X, Y and a are in their respective physical (unphysical) sheets.⁶ The contribution of F to σ is then proportional to

$$\sigma^F = \lim_{\epsilon \rightarrow 0} \int F_{ppp}(X, Y - i\epsilon, a) F_{ppp}^*(X, Y - i\epsilon, a) d\tau.$$

By inspection of the Feynman representation of F ,

$$F_{ppp}^*(X, Y - i\epsilon, a) = F_{ppp}(X, Y + i\epsilon, a)$$

and by continuity

$$F_{ppp}(X, Y + i\epsilon, a) = F_{ppp}(X, Y - i\epsilon, a).$$

So σ^F may be written as

$$\sigma^F = \lim_{\epsilon \rightarrow 0} \int F_{ppp}(Z, Y - i\epsilon, a) F_{ppp}(X, Y - i\epsilon, a) d\tau \quad (8)$$

which defines the continuation of σ^F for all Y .¹⁸

We are particularly interested in the cross sections σ_2 and σ_3 . Ascoli¹⁹ has shown that

$$\sigma_2 = f(s, W^2) (\partial x_{15} / \partial \Delta^2) \int |T|^2 d \cos \theta d \phi.$$

From (A15'), $\partial x_{15} / \partial \Delta^2$ has the form $g(s, W^2, \Delta^2) / (\epsilon_1^2 - m^2)^{3/2}$ where g is regular in Δ^2 , so that

$$\sigma_2 = [R(s, W^2, \Delta^2) / (\epsilon_1^2 - m^2)^{3/2}] \int |T|^2 d \cos \theta d \phi,$$

where R is regular in Δ^2 . Apart from those of the integral, then, σ_2 has singularities at $\epsilon_1 = \pm m$, or $\Delta^2 = m^2 + s \pm 2m\sqrt{s}$. Also,

$$\sigma_3 = [R' / (\epsilon_1^2 - m^2)^2] \int |T|^2 d \phi$$

where R' is regular in Δ^2 , so that σ_3 has a second-order pole at $\epsilon_1 = \pm m$.

We ought now to rewrite $|T|^2$ in the appropriate way for (8), and use the usual technique^{5,6} for discussing the singularities of the integrals. In practice, this seems to be very awkward for the triangle graphs. As mentioned in Sec. 2C, if we integrate over $\cos \theta$ and ϕ , a nonlinear Δ^2 dependence in t and Q^2 is introduced via (A14) and (A15), considerably complicating matters. The results of Sec. 3 apply directly only to σ_4 , therefore, and to discuss the singularities of σ_4 we must find those of the various amplitudes on the unphysical sheets like ppp . This can be done using the technique of Bonnevey *et al.*,⁶ but will not be discussed further: We assume that Fig. 8 (and the symmetric one with 3 and 5 exchanged) still represents the most dangerous graph, and any other dangerous one is treated similarly.

Only the pole terms are easily handled. The $t = \mu^2$ pole has been discussed by Ascoli. Dropping the factor $R(\epsilon_1^2 - m^2)^{3/2}$, its contribution to σ_2 is

$$\sigma_2^{(14)} = 2\pi \int_{-1}^1 \frac{dz}{[-2q^2 - x + 2q^2(q^2 + x)^{1/2} - \mu^2 - i\epsilon]^2}, \quad (9)$$

using (A14'). The root is positive when x is real and $\geq -q^2$. As we saw in Sec. 2, the denominator vanishes along an arc of a circle in the x plane but no pinch occurs and only the end-point singularities remain: (9) integrates to give

$$\sigma_2^{(14)} = \left[\frac{4\pi}{4q^2(x + q^2) - (2q^2 + \mu^2 + x)^2} \right], \quad (10)$$

which has poles at $x = -\mu^2 \pm 2iq\mu$. $\sigma_2 - \sigma_2^{(14)}$ is free of these poles, though there will still be contributions from cross terms involving them.

If these interference terms are small, it is enough to consider the pole terms independently. Of these, the closest to $x = 0$ are those at S_{36} , $S_{46} = m^2$, and S_{45} , $Q^2 = m_d^2$, and the final-state interaction poles. Using (A14') and (A15), omitting the kinematical factors, and taking $q^2 = q_0^2$, the S_{36} pole contributes

$$\sigma_3^{(36)} = \frac{2\pi(a + bz)}{[(a + bz)^2 - c^2(1 - z^2)]^{3/2}}, \quad (11)$$

where

$$\begin{aligned} a &= -q_1^2 + p^2, \\ b &= \left(\frac{\frac{1}{4}q_1^2 - \alpha^2}{\frac{1}{4}q_1^2 + p^2} \right)^{1/2} (q_1^2 - p^2), \\ c &= \left(\frac{\frac{1}{4}q_1^2 - \alpha^2}{\frac{1}{4}q_1^2 + p^2} \right) p^2 (4q_1^2 - 9p^2)^{1/2}. \end{aligned}$$

¹⁸ See also reference 4.

¹⁹ R. Ascoli, *Nuovo Cimento* **18**, 744 (1960).

$\sigma_3^{(36)}$ is singular at $x=0$ for $z=+1$, and at $x\sim-0.9$, $x=0.4\pm 0.4i$ for $z=0$ (see Sec. 3A). Similarly, the contribution to σ_2 is

$$\sigma_2^{(36)} = \frac{4\pi}{a^2 - b^2 - c^2},$$

which is singular near $x=0$. These results hold for the S_{46} pole if we change the sign of z .

The Q^2 and S_{45} poles are of the same type, though we argued in Sec. 3C that their effect is probably small. Using (A15), we find that $\sigma_3^{(Q^2)}$ is singular at $x=0$ for $Z=-1$, while $\sigma_2^{(Q^2)}$ is constant; exchange of 3 and 4 is effected by putting $-z$ for z .

The final-state interaction poles are of the form (6). The Q^2 term contributes to σ_3 a term proportional to $[(a'+b'z)^2 - c'^2(1-z^2)]^{-1/2}$, where

$$\begin{aligned} a' &= \frac{1}{2}q_1^2 - \alpha^2 + 4/a_s^2, \\ b' &= -\left(\frac{\frac{1}{4}q_1^2 - \alpha^2}{\frac{1}{4}q_1^2 + p^2}\right)^{1/2} (\frac{1}{2}q_1^2 - p^2), \\ c' &= -c. \end{aligned}$$

It is singular at $x=0$ for $z=\pm 1$, neglecting α^2 . Its contribution to σ_2 is proportional to

$$\frac{1}{q_0} \ln \frac{\{a_s(q_1^2 q_0^2 + a'b') + [4c'q_1^2 + a_s^2(q_0^2 q_1^2 + a'b')^2]^{1/2}\}}{\{a_s(-q_1^2 q_0^2 + a'b') + [4c'q_1^2 + a_s^2(-q_0^2 q_1^2 + a'b')^2]^{1/2}\}}, \quad (12)$$

which is singular near $x=0$.

The result is true for the other final-state interaction. As expected, these are the most troublesome singularities; in an extrapolation of σ_2 , one should include a term of the form (12) in the fitting curve, which allows for these dominant effects explicitly. In fact, one might sum up the results of this, and the previous, section by saying that extrapolation to partial cross sections seems likely to be more successful than extrapolation to total cross sections. This is because each integration leads to the inclusion of "dangerous" phase-space points—regions for which the various singularities approach closest to the C-L pole. Only for σ_4 it is possible to avoid this trouble entirely.

5. CONCLUSIONS

The results of the last section must now be translated into experimental terms. The cross sections σ_2 , σ_3 , and σ_4 have to be related to measured quantities, kinematic singularities located, and dangerous regions of phase space avoided; also, one has to consider what is the most convenient way of collecting the data. In this section we discuss, in particular, the experiment of Griffiths, in which the two protons are detected in coincidence.

The cross section is²⁰

$$d\sigma = \frac{1}{v_1} \frac{2\pi |T|^2 \rho}{2E_1 2m_d}, \quad (13)$$

where

$$\begin{aligned} \rho &= \frac{1}{2\pi} (2\pi)^4 \delta^4(p_1 - p_6 - p_3 - p_4 - p_5) \\ &\quad \times \prod_{i=3}^5 2\pi \delta(p_i^2 - m^2) \theta(p_{i0}) \frac{d^3 p_i}{(2\pi)^4}, \end{aligned}$$

and $v_1 = q_1/m$. We fix the normalization of T below. Equation (13) gives²¹

$$\Sigma_4 = \frac{\partial \sigma}{\partial |\mathbf{p}_4| \partial z_{13} \partial z_{14} \partial \varphi_{34}} = \frac{A |T|^2 |\mathbf{p}_3|^3 |\mathbf{p}_4|^2}{E_4 E_{134}},$$

where $A = 2\pi/v_1 E_1 m_d (2\pi)^5$ and $E_{134} = \mathbf{p}_3^2 (W - E_4) - E_3 \mathbf{p}_3 \cdot (\mathbf{q}_1 - \mathbf{p}_4)$. The measured cross section Σ_4 has to be related to σ_4 , via the Jacobian $J = \partial(|\mathbf{p}_4| z_{13} z_{14} \varphi_{34}) / \partial(st\Delta^2 Q^2)$. This is done in Appendix B, Eq. (B1).

All particles are coplanar, so we need $\partial \sigma_3 / \partial \varphi_{34}$, $\partial \sigma_2 / \partial \varphi_{34}$ with $\varphi_{34} = \pi$. Since

$$\frac{\partial z_{34}}{\partial \varphi_{34}} = (-k_{134})^{1/2} \quad \text{and} \quad \frac{\partial Q^2}{\partial z_{34}} = \frac{2|\mathbf{p}_3||\mathbf{p}_4|m_d}{E_{34}},$$

where

$$E_{34} = (E_4 - E_3) + \left(\frac{|\mathbf{p}_3| E_4}{|\mathbf{p}_4|} - \frac{|\mathbf{p}_4| E_3}{|\mathbf{p}_3|} \right) z_{34}, \quad (15)$$

where k_{134} is defined in Appendix B we have

$$\partial \sigma_3 / \partial \varphi_{34} = E_4 E_{134} \Sigma_4 / 8m_d q_1^2 E_{34} |\mathbf{p}_3|^3 |\mathbf{p}_4|^2 \quad (16)$$

$$= A |T|^2 / 8m_d q_1^2 E_{34}. \quad (17)$$

Kinematic singularities appear in $\partial \sigma_3 / \partial \varphi_{34}$ at $E_{34} = 0$; by inspection, this occurs when $\mathbf{p}_3 = \mathbf{p}_4$, which from (A22) is at $p^2 = 0$ or $(4/9)q_1^2$ for $z=0$, $q^2 = q_0^2$. So $E_{34}(\partial \sigma_3 / \partial \varphi_{34})$ must be extrapolated.

The extrapolation is done at constant t and s , so we must specify how to move in $(E_4 z_{13} z_{14})$ space in order to travel on the line $L: (s, t = \text{constant})$ in $(st\Delta^2)$ space in such a way that p^2 decreases to zero. If, equivalently, we keep z fixed, we can use (A22) and (A23) to find E_4 , z_{13} and z_{14} for fixed z and q^2 , and various p^2 . (It seems unlikely that the resulting redundancy of t changes the conclusions of Sec. 3 very much; it can easily be included

²⁰ R. P. Feynman, *Theory of Fundamental Processes* (W. A. Benjamin, Inc., New York, 1961), p. 73 ff.

²¹ Compare Eq. (9) of reference 3.

in the pole terms, as we saw). Plots of (A22), (A23) for $q^2=q_0^2$, $z=0, \frac{1}{4}, \frac{1}{2}$ are shown in Figs. 10(a) and (b). For a chosen z , the values of E_3, E_4, z_{13} , and z_{14} corresponding to various p^2 values can be read off. These graphs show how to select regions of phase space near $z=0$. Similar plots can be made for constant t .

Consider first an experiment in which t is fixed. At each point on L, Σ_4 is determined experimentally, and hence from (15) and (16), $E_{34}(\partial\sigma_3/\partial\varphi_{34})$ is calculated. On L everything is a function of p^2 only, so that we have, say, six to ten numbers to extrapolate to $x=0$. We suggested in Sec. 4 that a possible choice for the fitting curve would be to take for $|T|^2$

$$|T|^2 = \frac{S}{(\Delta^2 - m^2)^2} + \frac{\beta}{(\Delta^2 - m^2)} + \gamma \left(\frac{1}{Q^2 + 1/a^2} + \frac{1}{\frac{1}{4}(p_4 - p)^2 + 1/a^2} \right) + \text{power series in } p^2, \quad (18)$$

where S is a function of s and t , and β and γ are constants. The coefficient S is to be found; [notice that everything appearing in $\partial\sigma_3/\partial\varphi_{34}$ given by (17) with (18) for $|T|^2$ is measured]. Substituting the first term of (18) into (13), taking the nonrelativistic limit and comparing with Eq. (2.4) of C-L, we get the relation between S and the p - p differential cross section $\partial\sigma/\partial\Omega$:

$$S = [8m2\alpha/(1-r_0\alpha)\pi v_1 A][\partial\sigma/\partial\Omega],$$

where r_0 is the triplet effective range. We also note that according to Singh's estimate,¹⁶ γ should be roughly 7 times S .

If we keep $\cos\theta$ fixed, we have to calculate $\partial\sigma_2/\partial\cos\theta\partial\varphi_{34}$. We have

$$\frac{\partial\sigma_2}{\partial\cos\theta\partial\varphi_{34}} = \frac{\partial\sigma_3}{\partial\varphi_{34}} \frac{q}{2\sqrt{s}} [(s+m^2-\Delta^2)^2 - 4m^2s]^{1/2},$$

where $\partial\sigma_3/\partial\varphi_{34}$ is given by (16). As well as the kinematic singularity $E_{34}=0$, there are now branch points at $\Delta^2 = s + m^2 \pm 2m\sqrt{s}$, so one must extrapolate

$$\{E_{34}/[(s+m^2-\Delta^2)^2 - 4m^2s]^{1/2}\} [\partial\sigma_2/\partial\cos\theta\partial\varphi_{34}] = (q/2\sqrt{s})E_{34}(\partial\sigma_3/\partial\varphi_{34}),$$

which is related to measured quantities as before.

This way of extrapolating is wasteful of the data. If ten different p^2 values are chosen, one has to do several experiments at different settings of θ_{13}, θ_{14} . Suppose the counters have an angular spread of 2° . From Fig. 10(a), we see that if $z=0$, only $0 \leq p^2 \leq 0.08q_1^2$ can be covered; the value of p^2 being found by following the $z=0$ line for p_3^2 or p_4^2 in Fig. 10(b). To cover the range $0 \leq p^2 \leq 0.16q_1^2$, three angle settings are needed, and so on. On

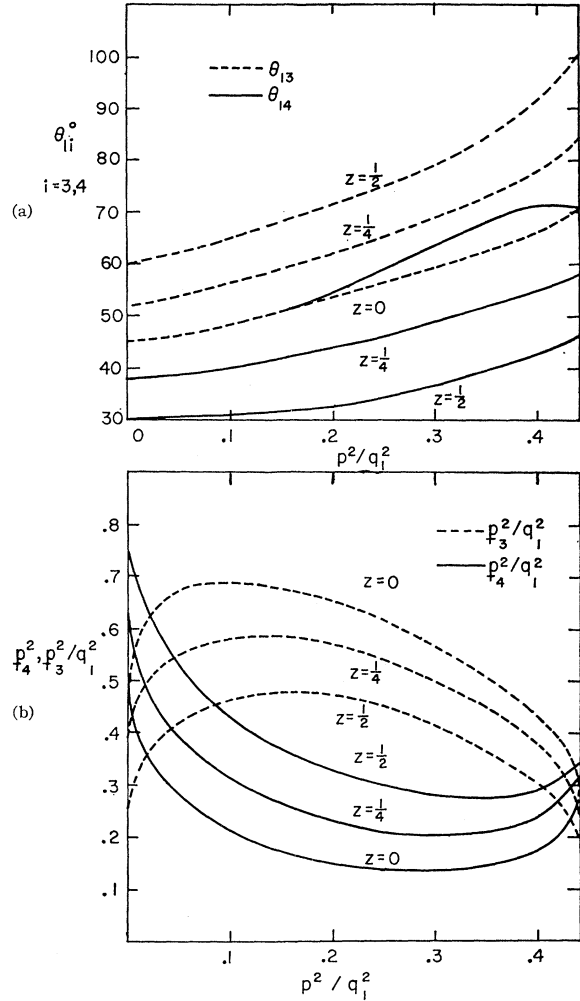


FIG. 10. The correspondence between laboratory variables and p^2, z .

the other hand, the $z=1/2$ curve for θ_{14} rises very slowly, and the angle would not have to be changed for this z to obtain the range $0 \leq p^2 \leq 0.2q_1^2$. For each setting, a spectrum of energies is recorded though only one point is used, corresponding to the chosen p^2 . The data could be used to better advantage if the form (18) were modified to include terms in q^2 and z , so that the complete energy spectrum at each angle could be fitted. The two procedures would in any case complement each other.

Finally, σ_2 can be measured directly by measuring the energy and angle of the recoil particle 5, since from (A1)

$$\sigma_2 = \frac{1}{4q_1 p} \frac{\partial\sigma}{\partial p^2 \partial z_{15}}$$

The fact that z_{15} , not q^2 , is the free variable introduces complications into the analysis of Secs. 3 and 4, which would have to be reconsidered.

ACKNOWLEDGMENTS

The bulk of this work was done while the author was the recipient of a D.S.I.R. Research Studentship, at the Department of Mathematical Physics, The University of Birmingham. It is a pleasure to thank Professor R. E. Peierls for his kind interest and help. I also thank Dr. R. J. Eden for suggesting this problem, Dr. L. Castillejo for valuable advice and suggestions and Dr. R. J. Griffiths for enlightening conversations and correspondence about the experimental arrangement.

APPENDIX A

We derive a number of kinematical results used in the text.

1. The Physical Regions

With the notation of Sec. 2,

$$2\mathbf{q}_1 \cdot \mathbf{p} = s - W^2 - \Delta^2 + m_d^2 + 2E_1E_5$$

so that

$$2q_1 p_{z15} = 3p^2 + 4(q^2 + \alpha^2) - q_1^2, \quad (\text{A1})$$

and $|z_{15}| \leq 1$ leads to the C-L phase diagram. Again,

$$2\mathbf{q}_1 \cdot \mathbf{p}_4 = t - 2m^2 + 2E_1E_4 \quad (\text{A2})$$

and

$$2\mathbf{q}_1 \cdot \mathbf{p}_3 = m^2 + \Delta^2 - t - s + 2E_1E_3, \quad (\text{A3})$$

where $2m_dE_3 = Q^2 + \Delta^2 - t - m^2$, $2m_dE_4 = t + W^2 - Q^2 - m^2$, $2m_dE_1 = W^2 - m^2 - m_d^2$. In terms of (\mathfrak{U})

$$E_3 = m + \mathbf{p}_3^2/2m = m + \mathbf{Q}^2/m - p^2/2m - t/4m, \quad (\text{A5})$$

and

$$E_4 = m + \mathbf{p}_4^2/2m = m - \mathbf{Q}^2/m + \mathbf{q}_1^2/2m + t/4m - \alpha^2/m. \quad (\text{A6})$$

For $q^2 = q_0^2$, $|z_{14}|$ becomes

$$4q_1^2(2\mathbf{Q}^2 - p^2 - t/2) - \left[3p^2 - \frac{3t}{2} - 2(\mathbf{Q}^2 + \alpha^2) \right]^2 \geq 0. \quad (\text{A7})$$

Using (A2) and (A4), $|z_{14}| \leq 1$ is

$$4q_1^2[t/2 - q_1^2 - 2(\mathbf{Q}^2 + \alpha^2)] - \left[2q_1^2 + \frac{3t}{2} - 2(\mathbf{Q}^2 + \alpha^2) \right]^2 \geq 0. \quad (\text{A8})$$

2. Redundancy Relations

The four-momentum conservation relation is

$$\mathbf{p}_1 + \mathbf{p}_6 = \mathbf{p}_3 + \mathbf{p}_4 + \mathbf{p}_5.$$

Squaring,

$$S_{45} = W^2 - s - Q^2 + m_3^2 + m_4^2 + m_5^2. \quad (\text{A9})$$

Defining

$$\tilde{t} = S_{13} = (p_1 - p_3)^2, \text{ we have } s + t + \tilde{t} = \Delta + m_3^2 + m_4^2 + m_1^2,$$

which yields

$$\tilde{t} = \Delta^2 - s - t + m_1^2 + m_3^2 + m_4^2. \quad (\text{A10})$$

Since $Q^2 = W^2 - 2\mathbf{p}_1 \cdot \mathbf{p}_4 - 2\mathbf{p}_4 \cdot \mathbf{p}_6 + m_4^2$,

$$S_{46} = Q^2 - t - W^2 + m_1^2 + m_4^2 + m_6^2, \quad (\text{A11})$$

and squaring $(p_1 + p_6 - p_3) = (p_4 + p_5)$, with (A9) and (A10) we get

$$S_{36} = t - Q^2 - \Delta^2 + m_3^2 + m_5^2 + m_6^2. \quad (\text{A12})$$

Finally, using (A11) and (A12),

$$S_{15} = s - W^2 - \Delta^2 + m_1^2 + m_5^2 + m_6^2. \quad (\text{A13})$$

The expressions connecting t , Q^2 with θ and φ are obtained as follows. In the 3-4 c.m. system, denote the initial and final three-momenta by \mathbf{r} and \mathbf{q} , and write $w_r^2 = m^2 + \mathbf{r}^2$, $w_q^2 = m^2 + \mathbf{q}^2$, ($r = |\mathbf{r}|$, $q = |\mathbf{q}|$), then $S = 4w_q^2$, $t = 2m^2 - 2w_q w_r + 2qr \cos\theta$, $\tilde{t} = 2m^2 - 2w_q w_r - 2qr \times \cos\theta$. Hence, $t + \tilde{t} = 4m^2 - 4w_q w_r = 3m^2 + \Delta^2 - s$ from (A10), so that we obtain

$$t = 2m^2 - \frac{1}{2}(m^2 + s - \Delta^2) + \cos\theta \left[(s - 4m^2)/s \right]^{1/2} \times \left[(s + m^2 - \Delta^2)^2 - 4sm^2 \right]^{1/2}. \quad (\text{A14})$$

We note that $r^2 = p^2 + q^2 + \alpha^2$, so that also we have

$$t = -q^2 - r^2 + 2qz = -2q^2 - p^2 - \alpha^2 + 2qz(p^2 + q^2 + \alpha^2)^{1/2}. \quad (\text{A14}')$$

Let x_{ij} be the cosine of the angle between i and j , and let ϵ_i be the energy of i , all in the 3-4 c.m. system. Then we find

$$Q^2 = 2m^2 + 2\epsilon_3\epsilon_5 - 2[(\epsilon_3^2 - m^2)(\epsilon_5^2 - m^2)]^{1/2}x_{35}$$

and

$$x_{35} = x_{13}x_{15} + (1 - x_{13}^2)^{1/2}(1 - x_{15}^2)^{1/2} \cos\varphi.$$

x_{13} is just $-\cos\theta$. Using (A13), it follows that

$$x_{15} = \left[2\epsilon_1\epsilon_5 + s - W^2 - \Delta^2 + m_d^2 \right] / 2(\epsilon_1^2 - m^2)^{1/2} \times (\epsilon_5^2 - m^2)^{1/2} \quad (\text{A15})$$

and the ϵ_i are

$$2s^{1/2}\epsilon_i = (s + m^2 - \Delta^2), \quad 2\epsilon_3 = s^{1/2}, \quad 2s^{1/2}\epsilon_5 = W^2 - s - m^2.$$

In terms of (\mathfrak{U}) , we have

$$x_{15} = (-q_1^2 - \alpha^2 + 3x + q^2) / 2(q^2 + x)^{1/2} [q_1^2 - 3(q^2 + \alpha^2)]^{1/2}.$$

For $q^2 = q_0^2$, it follows that

$$4\mathbf{Q}^2 = q_1^2/2 - \alpha^2 - \left(\frac{\frac{1}{4}q_1^2 - \alpha^2}{\frac{1}{4}q_1^2 + p^2} \right)^{1/2} \{ (q_1^2/2 - 3p^2)z + \cos\varphi [p(4q_1^2 - qp^2)^{1/2}(1 - z^2)^{1/2}] \}. \quad (\text{A15}')$$

The root is certainly real, since $0 \leq p^2 \leq 4/9q_1^2$. The coplanar case is expressed by $\varphi_{34} = \pi$, or equivalently by

$$\theta_{13} + \theta_{14} = \theta_{34}, \quad (\text{A16})$$

where θ_{ij} is the laboratory angle between i and j . (A16) may be written as

$$2q_1^2 \mathbf{p}_3 \cdot \mathbf{p}_4 = 2\mathbf{p}_3 \cdot \mathbf{q}_1 2\mathbf{p}_4 \cdot \mathbf{q}_1 - [4p_3^2 q_1^2 - (2\mathbf{p}_3 \cdot \mathbf{q}_1)^2]^{1/2} \times [4p_4^2 q_1^2 - (2\mathbf{p}_4 \cdot \mathbf{q}_1)^2]^{1/2}. \quad (\text{A17})$$

Also, we have

$$2\mathbf{p}_3 \cdot \mathbf{p}_4 = 2m^2 + 2E_3 E_4 - s. \quad (\text{A18})$$

Equation (A17) is then given in terms of (\mathfrak{X}) using (A2) and (A4); for $q^2 = q_0^2$, neglecting α^2 , (A17) is

$$16\mathbf{Q}^4(4p^2 + q_1^2) + 8\mathbf{Q}^2(q_1^2 t - 6p^2 t - 6p^4 - 4q_1^2 p^2) + q_1^2(t + 4p^2)^2 = 0. \quad (\text{A19})$$

At $\mathbf{Q}^2 = 0$, (A19) is just $t = -4p^2$, or

$$z = (q_1^2/2 - 3p^2)/q_1(p^2 + q_1^2/4)^{1/2}, \quad (\text{A20})$$

which checks with (A15) for $\mathbf{Q}^2 = 0$. If, in (A17), we put $\mathbf{Q}^2 = 0$ and neglect α^2 , we find

$$t^2[4q_1^4 - 12p^2 q_1^2] + t[-48p^2 q^2 q_1^2 + 20p^2 q_1^4 - 4q_1^6 - 64q_1^2 q^4 + 32q^2 q_1^4] + 16p^4 q_1^4 = 0. \quad (\text{A21})$$

3. Relations Between the Laboratory and (\mathfrak{X}) Variables

To see how to select experimentally regions of phase space defined in terms of (\mathfrak{X}) variables, we solve for \mathbf{p}_3^2 , \mathbf{p}_4^2 , z_{13} , and z_{14} in terms of p^2 , q^2 , and z , putting $\varphi_{34} = \pi$. After tedious algebra, the result is

$$\mathbf{p}_3^2 = \frac{1}{2} \left\{ (q_1^2 - p^2 - 2\alpha^2) \frac{qz(q_1^2 - p^2)}{r} \pm \frac{q_1}{r} [4q^2 p^2 (1 - z_{15}^2)(1 - z^2)]^{1/2} \right\}, \quad (\text{A22})$$

$$\mathbf{p}_4^2 = q_1^2 - \mathbf{p}_3^2 - p^2 - 2\alpha^2,$$

$$2|\mathbf{p}_3| q_1 z_{13} = \frac{3}{2}(q_1^2 - p^2)$$

$$-2(q^2 + \alpha^2) - qz \left\{ 2r + \frac{q_1^2 - p^2}{2r} \pm \frac{q_1}{2r} [4q^2 p^2 (1 - z_{15}^2)(1 - z^2)]^{1/2} \right\}. \quad (\text{A23})$$

The expression for $2|\mathbf{p}_4| q_1 z_{14}$ is the same as (A23), the sign of z and the (\pm) being changed. z_{15} is given by (A1).

Since $\mathbf{Q} = \frac{1}{2}(\mathbf{p}_3 - \mathbf{p}_4)$, $\mathbf{Q}^2 = 0$ is

$$q_1^2 - 2q^2 - 3\alpha^2 + 2q^2 \left[r - \frac{(q_1^2 - p^2)}{2r} \right] = \frac{q_1}{r} [4q^2 p^2 (1 - z_{15}^2)(1 - z^2)]^{1/2}. \quad (\text{A24})$$

Substituting (A1) into (A24), putting $q^2 = q_0^2$ and neglecting α^2 , we recover (A20). If α^2 is included, we find, for example at $z=0$, $p^2 = q_1^2/6 \pm (4\alpha^2/9)i$, so that the point $q_1^2/6$ is shifted off the physical region by $O(\alpha^2)$; the same is true for the points $p^2=0$, $(4/9)q_1^2$.

APPENDIX B

Instead of $|\mathbf{p}_4|$ and φ_{34} it is convenient to use E_4 , and z_{34} defined by

$$z_{34} = z_{13} z_{14} + (1 - z_{13}^2)^{1/2} (1 - z_{14}^2)^{1/2} \cos \varphi_{34}.$$

Using (A2), (A3), and (A18) with (A4) we obtain

$$J' = \frac{\partial(E_4 z_{13} z_{14} z_{34})}{\partial(st\Delta^2 Q^2)} = \frac{E_{134}}{16m_d^2 q_1^2 \mathbf{p}_3^4 \mathbf{p}_4^2}.$$

At constant s , t , and Δ^2 , $\partial z_{34}/\partial \varphi_{34} = (-k_{134})^{1/2}$ where $-k_{134} = 1 - z_{13}^2 - z_{14}^2 - z_{34}^2 + 2z_{13} z_{14} z_{34}$, and of course $\partial E_4/\partial |\mathbf{p}_4| = |\mathbf{p}_4|/E_4$. Hence $\sigma_4 = J\Sigma_4$, where

$$J = \frac{E_4 E_{134}}{16m_d^2 q_1^2 |\mathbf{p}_4|^3 \mathbf{p}_3^4 (-k_{134})^{1/2}}. \quad (\text{B1})$$